Published in final edited form as:
J Phys Chem C Nanomater Interfaces. 2012 February 23; 116(7): 4493–4499. doi:10.1021/jp211722z.

Green, Silica-Coated Monoclinic Y_2O_3:Tb^{3+} Nanophosphors: Flame Synthesis and Characterization

Georgios A. Sotiriou, **Melanie Schneider**, and **Sotiris E. Pratsinis***
Particle Technology Laboratory, Institute of Process Engineering, Department of Mechanical and Process Engineering, Sonneggstrasse 3, CH-8092 Zurich, ETH Zurich, Switzerland

Abstract

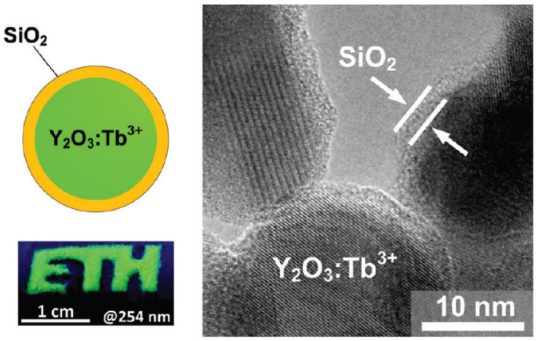

Silica-coated and uncoated, Tb-doped (1–5 at % Tb) Y_2O_3 green nanophosphors were made, for the first time, in a single step by flame aerosol technology with controlled crystal phase (cubic and monoclinic) and morphology. The nanophosphors were characterized by X-ray diffraction, N_2 adsorption, high resolution electron microscopy, and photoluminescence spectroscopy. The monoclinic crystal structure of Y_2O_3:Tb^{3+} nanophosphors favors the electric dipole $^5D_4 \rightarrow {}^7F_5$ transition driving their green phosphorescence. The phosphorescence of the SiO_2-coated monoclinic Y_2O_3:Tb^{3+} nanophosphors is lower than the uncoated ones. Upon annealing these nanophosphors, they were transformed from monoclinic to cubic and their phosphorescence was reduced. This further indicates the superior performance of the monoclinic crystal phase for the electric dipole transitions of Tb^{3+} ions.

I. INTRODUCTION

Luminescent light-emitting nanoparticles have potential applications in high-definition displays,[1] lasers,[2] and bioimaging.[3] Among these particles, rare-earth phosphors doped with lanthanide ions have advantageous optical properties for their superior photostability.[4] Yttria (Y_2O_3) is one of the most studied ceramics as a host matrix, especially when doped with europium (Eu^{3+}), resulting in a bright red emission.[5] Furthermore, the emission color depends on the chosen dopant element.[6] For example, when Y_2O_3 is doped with terbium (Tb^{3+}), a bright green emission occurs.[5,7] In fact, the color of nanosized Y_2O_3 nanocrystals can be finely tuned from bright green to red by codoping them with Tb^{3+} and Eu^{3+} during their flame synthesis without altering their crystal and particle sizes by such doping.[8]

*Corresponding Author pratsinis@ptl.mavt.ethz.ch..

The authors declare no competing financial interest.

Europe PMC Funders Author Manuscripts

Such nanocrystals are particularly attractive for bioimaging, as they do not degrade during analysis (photobleaching) compared to organic dyes and are relatively nontoxic compared to semiconducting (e.g., CdSe, PbS) nanoparticles (quantum dots).[3,9] For such bioapplications, the nanoparticle surface often needs to be modified to increase its biocompatibility. Recently, it was shown that a dense nanothin silica layer[10,11] drastically minimized the toxicity of plasmonic nanosilver, as it prevented the release of toxic ions and the direct contact of nanosilver with human cells.[12] In fact, such a layer can facilitate surface biofunctionalization for specific molecule binding[10] and the dispersion of nanophosphors.[11]

The crystal structure and particle size of the host matrix (e.g., Y_2O_3) can influence the luminescent properties of nanophosphors.[13] For example, the luminescence of monoclinic Y_2O_3 doped with Eu^{3+} is lower than that of cubic Y_2O_3, so the luminescence of the latter has been studied extensively.[13-16] Monoclinic Y_2O_3 can be made efficiently also, especially at high temperatures and fast cooling rates.[13,17] In cubic Y_2O_3, there are two sites where rare earth ions can substitute Y^{3+}: one with C_2 symmetry and without any inversion center (75% of the sites) and one with S_6 symmetry with an inversion center.[18,19] In monoclinic Y_2O_3, all sites have C_s symmetry without any inversion center.[19] It has been shown theoretically as early as in 1967 that for green luminescence Tb^{3+} ions should be embedded in lattice sites without inversion symmetry, such as the monoclinic Y_2O_3.[20] Nevertheless, as the red emission of monoclinic Y_2O_3:Eu^{3+} is less intense than that of its cubic phase,[13] a few have investigated the luminescence of monoclinic Y_2O_3:Eu^{3+} nanoparticles[13,17,21,22] and even fewer have involved other lanthanides such as Tb^{3+}.[19,22,23]

Here, silica-coated and uncoated Y_2O_3:Tb^{3+} nanophosphors are made by flame aerosol technology with controlled size and crystal phase (cubic and monoclinic). Flame synthesis is attractive, as it typically yields high-purity crystalline nanoparticles.[13] The Tb-content ranges from 1 to 5 at %. The nanophosphors are characterized by X-ray diffraction, N_2 adsorption, and high-resolution electron microscopy and their optical properties by photoluminescence spectroscopy. The effect of Y_2O_3 crystallinity and silica coating on the luminescence of Y_2O_3:Tb^{3+} nanophosphors is investigated. The monoclinic Y_2O_3 nanophosphors are annealed up to 1100 °C for 10 h to monitor the influence of the resulting phase transition from monoclinic to cubic on their phosphorescence.

II. EXPERIMENTAL SECTION

SiO_2-coated monoclinic Y_2O_3:Tb^{3+} nanophosphors were made in an enclosed flame-spray reactor.[24] In brief, yttrium nitrate (Aldrich, 99.9%) was dissolved in a 1:1 by volume mixture of 2-ethylhexanoic acid (EHA, Riedel-de Haen, 99%) and ethanol (Alcosuisse) to form the precursor solution. Its molarity was kept constant at 0.5 M for Y metal. The Tb doping was achieved by adding 1–5 at % Tb nitrate (Aldrich, 99.9%) to the above solution. The Tb atomic fraction (at %) was defined with respect to the total metal ion concentration. The precursor solution was fed to the spray nozzle (5 mL/min) and dispersed by 5 L/min oxygen (PanGas, purity >99.9%) and sheathed by 40 L/min oxygen. The freshly formed core Y_2O_3:Tb^{3+} particles were coated in-flight by swirl injection of hexamethyldisiloxane (HMDSO, Sigma Aldrich, purity ≥99%) vapor with 15 L/min nitrogen (PanGas, purity >99.9%) at room temperature through a metallic ring with 16 equidistant openings. The ring was placed on top of a 20 cm long quartz glass tube (inner diameter 4.5 cm) based at the spray nozzle followed by another 30 cm long such tube.[24] The HMDSO vapor was supplied by bubbling 0.5 L/min N_2 at 9 °C through approximately 350 mL of liquid HMDSO in a 500 mL glass flask.[24] The SiO_2 fraction in the product particles was kept at 16.6 wt %, assuming HMDSO fed at saturation conditions.[24] The as-prepared nanophosphor particles were collected on a glass microfiber filter (Whatman GF6, 257 mm diameter). Uncoated monoclinic Y_2O_3:Tb^{3+} particles were made under identical conditions as the above, in the

absence, however, of HMDSO vapor. Uncoated cubic Y_2O_3:Tb^{3+} nanophosphors were made[8] by feeding 11.6 mL/min of the precursor solution to the spray nozzle and dispersed to a fine spray by 3 L/min oxygen without any enclosure.

X-ray diffraction (XRD) patterns were recorded by a Bruker AXS D8 Advance diffractometer (40 kV, 40 mA, Cu Kα radiation) at 2θ = 20–70° with a step size of 0.03°. The obtained spectra were fitted using the TOPAS 3 software (Bruker) and the Rietveld fundamental parameter refinement.[13] High resolution transmission electron microscopy (HR-TEM) was performed with a CM30ST microscope (FEI; LaB6 cathode, operated at 300 kV, point resolution ~2 Å). Product particles were dispersed in ethanol and deposited onto a perforated carbon foil supported on a copper grid. Their photoluminescence was characterized at room temperature using a fluorescence spectrophotometer (Varian Cary Eclipse) containing a Xe flash lamp with tunable emission wavelength. Samples of 30 ± 2 mg were filled in a cylindrical substrate holder of 10 mm diameter and pressed toward a quartz glass front window. Emission spectra were recorded at 450–650 nm and excitation spectra at 200–400 nm with a step size of 0.5 nm. The decay time of the luminescence emission was determined by time-resolved measurements of the luminescence intensity with a resolution of 0.11 ms. Software supplied by Varian fitted exponential decay curves into the measured data points. Annealing of the samples was performed at 750, 850, 900, and 1100 °C for 10 h in an oven (Carbolite, CWF 1300) in air at ambient pressure.

III. RESULTS AND DISCUSSION

Morphology and Crystallinity of Y_2O_3:Tb^{3+} Nanoparticles

Figure 1 shows HR-TEM images at two magnifications of uncoated Y_2O_3:Tb^{3+} (2 at % Tb) nanoparticles made by open (a, d) and enclosed (b, e) spray flames, in which the crystal planes of the Y_2O_3 matrix can be seen.[8] For the uncoated Y_2O_3 from the open flame (a, d), there are both spherical and rhomdohedrally shaped particles,[13] while, for the Y_2O_3 made by the enclosed flame (b, e), there are mostly spherical. For the SiO_2-coated nanoparticles made by the enclosed flame (c, f), a smooth amorphous SiO_2 layer of about 2 nm encapsulates the crystal core, as with SiO_2-coated TiO_2,[24] Fe_2O_3,[25] and Ag[11] nanoparticles.

Figure 2 shows the XRD spectra of the Y_2O_3:Tb^{3+} (2 at %) nanoparticles of Figure 1. The ones made in open flames are mostly cubic (89%), in agreement with the literature[8,26] at these conditions (11.6 mL/min precursor solution feed rate, 3 L/min dispersion gas flow rate). The Y_2O_3 nanoparticles made by the enclosed flame, however, have only a minimal cubic fraction (<10%) and exhibit the characteristic pattern of the monoclinic phase.[27] Additionally, the presence of the SiO_2 coating does not significantly influence nanoparticle crystallinity,[25] as the XRD patterns of uncoated and SiO_2-coated nanoparticles are almost identical. The average crystal sizes (Figure 2, inset) of nanoparticles made by open (from now on, *cubic* Y_2O_3) and enclosed flame (from now on, *monoclinic* Y_2O_3) are similar for all three conditions, which facilitates their further luminescent evaluation, as shown later on.

Phosphorescence of Cubic and Monoclinic Y_2O_3:Tb^{3+} Nanoparticles

Figure 3a shows the excitation spectra of uncoated cubic[8] (solid line), uncoated monoclinic (broken line), and SiO_2-coated monoclinic (dotted line) Y_2O_3:Tb^{3+} (2 at % Tb) nanoparticles monitoring their emission at 545 nm. The cubic Y_2O_3:Tb^{3+} nanoparticles have a dominant band centered around 280 nm and a secondary band centered around 310 nm.[5,9,28] The monoclinic Y_2O_3:Tb^{3+} have the dominant band centered also around 280 nm but the secondary excitation band around 265 nm. These bands are assigned for the Tb^{3+} transitions within the phosphor particles.[28] This is the first indication that the crystal phase of the Y_2O_3 host matrix influences the luminescent properties.

This can be verified in the emission spectra (Figure 3b) of these nanoparticles when excited at 276 nm.[9] The strongest emission band from the electric dipole transitions of Tb^{3+} is typically located around 550 nm ($^5D_4 \rightarrow {}^7F_5$)[9,29] (a major peak at ~545 nm and a secondary peak at ~555 nm) corresponding to green color, and one around 490 nm ($^5D_4 \rightarrow {}^7F_6$) corresponding to blue.[9,20,29] The strongest emission of monoclinic Y_2O_3:Tb^{3+} is shifted to 547 nm (broken and dotted lines, Figure 3b). This shift could be attributed to symmetry changes at the cationic sites where the Tb^{3+} can substitute in the two different Y_2O_3 crystal phases.[5] Additionally, the intensity of the secondary peak at ~555 nm has decreased significantly when compared to the dominant one at 547 nm. Such spectrum characteristics have been obtained also by monoclinic Y_2O_3:Tb^{3+} phosphors.[23] The intensity of the band at ~490 nm has decreased also when compared to that at 547 nm. When the three emission spectra of Figure 3b are compared, the intensity around 545 nm of the monoclinic Y_2O_3 (broken line) is quite higher than that of the cubic (solid line).

Figure 4a shows the maximum phosphorescence intensities of these nanophosphors as a function of Tb content. The highest intensity is obtained for a Tb content of 2–4 at % regardless of Y_2O_3 crystal phase or SiO_2 coating, resulting from the increasing number of luminescent centers.[30] Above 4 at % Tb content, energy transfer between adjacent luminescent centers to inactive sites occurs, leading to phosphorescence quenching.[31] The uncoated monoclinic (open triangles) Y_2O_3:Tb^{3+} has higher phosphorescence for all Tb contents than both SiO_2-coated monoclinic (filled triangles) and uncoated cubic[8] (open circles) Y_2O_3 nanophosphors. The uncoated monoclinic nanophosphors have stronger phosphorescence than the SiO_2-coated ones, most probably by the UV-light absorption and scattering[32] of amorphous SiO_2 that reduces the excitation irradiation intensity. The SiO_2-coated monoclinic Y_2O_3:Tb^{3+} nanoparticles still outperform the uncoated cubic ones. This enables such biocompatible and easily dispersible nanoparticles to be employed in bioapplications without any adverse toxic effects, common with other light emitting nanoparticles that contain heavy metals (quantum dots).

Figure 4b shows the decay profiles of the uncoated and SiO_2-coated monoclinic Y_2O_3:Tb^{3+} (2 at % Tb) nanophosphors. Both profiles are similar, exhibiting the characteristic single exponential decay and indicating that the presence of the thin SiO_2 shell does not significantly influence the luminescence of the core Y_2O_3:Tb^{3+} particles. The exponential decay time constants of luminescence for both as-prepared uncoated and SiO_2-coated monoclinic Y_2O_3:Tb^{3+} (1–5 at %) nanophosphors had similar values and decreased from 2.72 to 1.66 ms for increasing Tb content and were slightly larger than those of cubic Y_2O_3:Tb^{3+} (from 2.67 to 1.09 ms)[8] and in agreement with flame-made Y_2O_3:Eu^{3+} nanophosphors of similar sizes.[13]

For both uncoated nanophosphors (monoclinic and cubic), however, the maximum intensity achieved by the monoclinic (broken line, open triangles) Y_2O_3 was about thrice higher than that of cubic (solid line, open circles). This suggests that monoclinic Y_2O_3 favors the green emission from the Tb^{3+} ions. This is in contrast to the red emission from the Eu^{3+} activated Y_2O_3 ($^5D_0 \rightarrow {}^7F_2$)[13] for which cubic Y_2O_3 is favorable. This emphasizes the effect of dopant composition on the luminescence of nanophosphors. The above result here is also in contrast to Y_2O_3:Tb^{3+} nanoparticles ~20–40 nm in diameter made by microemulsion[22] and showing higher phosphorescence intensity for cubic than monoclinic Y_2O_3. This lower phosphorescence for monoclinic Y_2O_3 was attributed to the presence of volatile impurities that were formed during its wet synthesis.[22] These impurities disappeared for higher annealing temperature and transformation of the monoclinic phase to the cubic.[22] Thus, the low degree of crystallinity and the presence of impurities in wet-made nanophosphors hindered phosphorescence by monoclinic Y_2O_3:Tb^{3+}. However, flame processes typically yield high-purity products[33] with desired crystallinity[13] that facilitate their luminescence.

Annealing of Uncoated and SiO_2-Coated Monoclinic Y_2O_3:Tb^{3+} Nanoparticles

To further evaluate the effect of crystal structure on the luminescence of Y_2O_3:Tb^{3+} nanophosphors, an annealing study of the monoclinic Y_2O_3 nanoparticles was performed. Figure 5a shows the XRD patterns of uncoated monoclinic Y_2O_3:Tb^{3+} (2 at % Tb) annealed at 750, 850, 900, and 1100 °C for 10 h. The as-prepared monoclinic Y_2O_3 transforms completely to cubic above 850 °C consistent with the literature.[22,27,34] With increasing temperature, the cubic phase is obtained while the estimated cubic crystal size increases from ~36 to ~90 nm, in line with the literature.[27]

The SiO_2-coated Y_2O_3:Tb^{3+} nanoparticles (Figure 5b) retain their mostly monoclinic phase until 850 °C as well as their crystal size (d_{XRD} = 22.5–25 nm), in contrast with the uncoated ones (Figure 5a). This indicates that the SiO_2 shell inhibits the core crystal growth during annealing, as seen with silica-coated nanosilver.[11] At 900 °C and above, a significant change in the XRD spectrum is observed. Apart from the formation of cubic Y_2O_3, also a few more peaks emerge (2θ = 23.3, 24.8, 26.7, 29.7, 30.8, 32.5, 46.2, 52.2, and 54.0°) that correspond neither to monoclinic nor cubic Y_2O_3 (Figure 5b, stars). These peaks most probably correspond to yttrium-silicates[35] that were formed by the interaction of the SiO_2 shell with the core crystal Y_2O_3 at this high temperature. This inhibits also the accurate estimation of the cubic and monoclinic crystal sizes and their mass fractions from the XRD spectra for temperatures above 850 °C.

Figure 6a shows the specific surface area (SSA) as a function of annealing temperature for uncoated (open triangles) and SiO_2-coated monoclinic Y_2O_3:Tb^{3+} (filled triangles) for 2 at % Tb-content, respectively. For the uncoated, the SSA monotonically decreases with annealing temperature with the formation of sinter necks[27] (Figure 6b) and coalescence of particles, in agreement with the increase of crystal size (Figure 5a). The SSA for the SiO_2-coated sample remains fairly constant up to 850 °C, so there is no significant increase in grain size. This indicates that the SiO_2 coating inhibits the core crystal growth and has encapsulated fully the Y_2O_3 core particles. Furthermore, the SSA of the as-prepared, uncoated, and SiO_2-coated nanoparticles is practically the same, indicating that there are no separate SiO_2 nanoparticles formed that would lead to larger SSA values.[24] For temperatures above 850 °C, however, the SSA decreases significantly and formation of sinter necks occurs (Figure 6c). No amorphous phase is detected by TEM, verifying the formation of the larger cubic Y_2O_3 crystal phase and the yttrium-silicates, in agreement with XRD (Figure 5b).

Figure 7a,b shows the excitation and emission spectra, respectively, of the annealed uncoated monoclinic Y_2O_3:Tb^{3+} (2 at % Tb) nanophosphors. For increasing annealing temperature, the monoclinic crystals transform to larger cubic ones (Figures 5a and 6a). Therefore, both excitation and emission spectra shift from monoclinic to cubic Y_2O_3. Figure 7b also shows that the emission phosphorescence intensity decreases with increasing annealing temperature and phase transformation, further indicating that the monoclinic Y_2O_3 crystal phase favors the green phosphorescence of Tb^{3+}. Such a decrease in the phosphorescence for higher annealing temperatures has also been observed for other systems (SiO_2:Tb^{3+}) and has been attributed to the reduction of effective Tb^{3+} luminescent centers because of the formation of optically inactive Tb clusters.[36]

Perhaps there is a better distribution of Tb^{3+} in the monoclinic Y_2O_3 host matrix because of its smaller size than cubic, facilitating the Tb^{3+} radiative transitions.[36] Furthermore, the probability of the $^5D_4 \rightarrow {}^7F_5$ electric-dipole transition of Tb^{3+} (responsible for the green color emission) contains contributions from linear and third order terms of the crystal lattice.[20] Some of the crystal point groups in the cubic Y_2O_3 have no linear term, and therefore, a larger transition probability may be realized by embedding Tb^{3+} in lattice sites

with crystals having linear terms,[20] such as the monoclinic Y_2O_3 (with corresponding crystal point group C_s).[19]

The excitation spectra of the SiO_2-coated monoclinic Y_2O_3:Tb^{3+} (2 at % Tb) for increasing annealing temperature (Figure 7c) exhibit characteristic bands related to the monoclinic phase until 850 °C. This indicates that the SiO_2 coating prevents the Y_2O_3 phase transformation, in agreement with XRD (Figure 5b). However, for annealing above 850 °C, an excitation band arises at quite low wavelength (<250 nm), which becomes the dominant one at 900 and 1100 °C. This band is most probably attributed to the interaction of the SiO_2 coating with the core Y_2O_3:Tb^{3+} and the formation of yttrium-silicates. This band could be related to the excitation of the ^7D energy level in the Tb^{3+} ion.[36] Nonetheless, at 1100 °C, where there is cubic Y_2O_3:Tb^{3+} (Figure 5b), the excitation bands (centered at ~280 and ~310 nm) related to the cubic phase are also present.

This transformation from monoclinic to cubic can also be observed in the emission spectra of the SiO_2-coated nanophosphors (Figure 7d), in which the reduction of the dominant peak occurs for the highest annealing temperature. Furthermore, the highest intensity at ~545 nm is obtained at 850 °C. At this temperature, the monoclinic phase (Figure 5b) and core size (d_{XRD} = ~25 nm) are retained. Most likely annealing at this temperature has improved the core Y_2O_3:Tb^{3+} crystallinity and eliminated any Y_2O_3 crystal defects,[22] increasing the phosphorescence intensity.[27,37] This further indicates that monoclinic Y_2O_3 favors the Tb^{3+} phosphorescence.

Figure 8 shows the radiative exponential decay time constants of the uncoated (open triangles) and SiO_2-coated (filled triangles) Y_2O_3:Tb^{3+} (2 at % Tb) as a function of annealing temperature. The radiative decay time constants of both as-prepared nanophosphors are comparable, indicating a little effect on the luminescent properties by the SiO_2 shell of the core Y_2O_3:Tb^{3+} nanophosphors. For increasing annealing temperature, the radiative decay time constant of the uncoated nanophosphors decreases monotonically as their size increases,[27] in agreement with Figure 6. In contrast, the radiative decay time of the SiO_2-coated nanophosphors slightly increases and remains at about the same level until 900 °C. At 1100 °C, however, the radiative decay time constant reaches similar values for both nanophosphors.

Figure 9 shows the maximum phosphorescence intensity of uncoated (a) and SiO_2-coated (b) monoclinic Y_2O_3:Tb^{3+} (2 at % Tb) nanophosphors when excited at 276 nm at different annealing temperatures. For uncoated monoclinic nanophosphors (Figure 9a), the graph can be divided into two areas: one ≤750 °C in which there is no significant change and one >750 °C in which core crystal growth and phase transformation from monoclinic to cubic occurs and, thus, the maximum phosphorescence decreases. For the SiO_2-coated nanophosphors (Figure 9b), the phosphorescence increases up to 850 °C because there is an improvement of the monoclinic phase and possibly elimination of any crystal defects while the SiO_2 coating prevents crystal growth and phase transformation. Above 850 °C, a dramatic reduction in phosphorescence occurs that is attributed to formation of cubic Y_2O_3 and yttrium-silicates.

IV. CONCLUSIONS

Terbium-doped Y_2O_3 nanophosphors (1–5 at % Tb) were made by flame spray synthesis and were dry-coated in situ by thin silica films. The optimum Tb content was 2–4 at % for both cubic and monoclinic Y_2O_3 nanophosphors. For the first time, to the best of our knowledge, it is shown that the phosphorescence intensity is higher for monoclinic Y_2O_3 rather than cubic. By annealing monoclinic nanophosphors, their phosphorescence was reduced as they were transformed to cubic. The SiO_2 coating prevented the monoclinic core

particle growth and phase transformation until 850 °C, while their crystallinity was improved by annealing that increased their phosphorescence. Therefore, monoclinic Y_2O_3 favors the green phosphorescence of Tb^{3+} ions, in contrast to the phosphorescence of the well-studied Eu^{3+} ions where there is higher phosphorescence for the cubic crystal structure. This understanding may facilitate synthesis of bright green nanophosphors with a biocompatible coating suitable for display and bioimaging applications.

Acknowledgments

We thank Dr. Frank Krumeich (Electron Microscopy Center, ETH Zurich) for the electron microscopy analysis. Financial support by the Swiss National Science Foundation (No. 200020-126694) and European Research Council is kindly acknowledged.

REFERENCES

(1). Justel T, Nikol H, Ronda C. Angew. Chem., Int. Ed. 1998; 37:3085.
(2). Igarashi T, Ihara M, Kusunoki T, Ohno K, Isobe T, Senna M. Appl. Phys. Lett. 2000; 76:1549.
(3). Zhang F, Wong SS. ACS Nano. 2010; 4:99. [PubMed: 20041671]
(4). Feldmann C, Justel T, Ronda CR, Schmidt P. J. Adv. Funct. Mater. 2003; 13:511.
(5). Ropp RC. J. Electrochem. Soc. 1964; 111:311.
(6). Bunzli JCG, Piguet C. Chem. Soc. Rev. 2005; 34:1048. [PubMed: 16284671]
(7). Anh TK, Ngoc T, Nga PT, Bich VT, Long P, Strek W. J. Lumin. 1988; 39:215.
(8). Sotiriou GA, Schneider M, Pratsinis SE. J. Phys. Chem. C. 2011; 115:1084.
(9). Das GK, Tan TTY. J. Phys. Chem. C. 2008; 112:11211.
(10). Sotiriou GA, Hirt AM, Lozach PY, Teleki A, Krumeich F, Pratsinis SE. Chem. Mater. 2011; 23:1985.
(11). Sotiriou GA, Sannomiya T, Teleki A, Krumeich F, Vörös J, Pratsinis SE. Adv. Funct. Mater. 2010; 20:4250.
(12). Sotiriou GA, Pratsinis SE. Environ. Sci. Technol. 2010; 44:5649. [PubMed: 20583805]
(13). Camenzind A, Strobel R, Pratsinis SE. Chem. Phys. Lett. 2005; 415:193.
(14). Konrad A, Fries T, Gahn A, Kummer F, Herr U, Tidecks R, Samwer K. J. Appl. Phys. 1999; 86:3129.
(15). Konrad A, Herr U, Tidecks R, Kummer F, Samwer K. J. Appl. Phys. 2001; 90:3516.
(16). Ray S, Pramanik P, Singha A, Roy A. J. Appl. Phys. 2005; 97:094312.
(17). Qin X, Ju YG, Bernhard S, Yao N. J. Mater. Res. 2005; 20:2960.
(18). Dhanaraj J, Jagannathan R, Kutty TRN, Lu CH. J. Phys. Chem. B. 2001; 105:11098.
(19). Gozzi D, Latini A, Salviati G, Armani N. J. Appl. Phys. 2006; 99:123524.
(20). Hoshina T. Jpn. J. Appl. Phys. 1967; 6:1203.
(21). Wang L, Pan YX, Ding Y, Yang WG, Mao WL, Sinogeikin SV, Meng Y, Shen GY, Mao HK. Appl. Phys. Lett. 2009; 94:061921.
(22). Graeve OA, Corral JO. Opt. Mater. 2006; 29:24.
(23). Ishiwada N, Ueda T, Yokomori T. Luminescence. 2011; 26:381. [PubMed: 20737651]
(24). Teleki A, Heine MC, Krumeich F, Akhtar MK, Pratsinis SE. Langmuir. 2008; 24:12553. [PubMed: 18850688]
(25). Teleki A, Suter M, Kidambi PR, Ergeneman O, Krumeich F, Nelson BJ, Pratsinis SE. Chem. Mater. 2009; 21:2094.
(26). Kubrin R, Tricoli A, Camenzind A, Pratsinis SE, Bauhofer W. Nanotechnology. 2010; 21:225603. [PubMed: 20453290]
(27). Camenzind A, Strobel R, Krumeich F, Pratsinis SE. Adv. Powder Technol. 2007; 18:5.
(28). Meng QY, Chen BJ, Xu W, Yang YM, Zhao XX, Di WH, Lu SZ, Wang XJ, Sun JS, Cheng LH, Yu T, Peng Y. J. Appl. Phys. 2007; 102:093505.
(29). Ray S, Patra A, Pramanik P. Opt. Mater. 2007; 30:608.

(30). Blasse G. Mater. Chem. Phys. 1987; 16:201.
(31). Blasse, G.; Grabmaier, BC. Luminescent Materials. Springer; Berlin: 1994.
(32). Fu Y-X, Sun Y-H. J. Alloys Compd. 2009; 471:190.
(33). Pratsinis SE. AIChE J. 2010; 56:3028.
(34). Zhang P, Navrotsky A, Guo B, Kennedy I, Clark AN, Lesher C, Liu QY. J. Phys. Chem. C. 2008; 112:932.
(35). Rakov N, Amaral DF, Guimaraes RB, Maciel GS. J. Appl. Phys. 2010; 108:073501.
(36). Sun JM, Skorupa W, Dekorsy T, Helm M, Rebohle L, Gebel T. J. Appl. Phys. 2005; 97:123513.
(37). Pradhan AK, Zhang K, Mohanty S, Dadson J, Hunter D, Loutts GB, Roy UN, Cui Y, Burger A, Wilkerson AL. J. Appl. Phys. 2005; 97:023513.

Europe PMC Funders Author Manuscripts

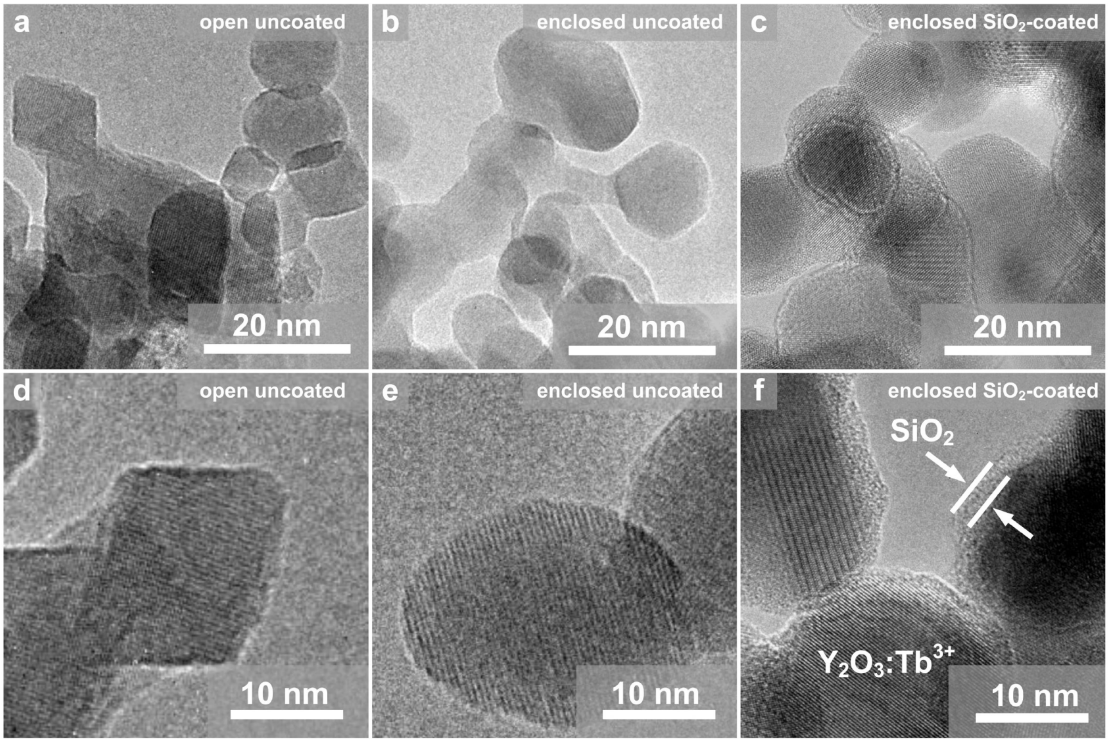

Figure 1.
High-resolution transmission electron microscopy images from the open uncoated (a, d), enclosed uncoated (b, e), and enclosed SiO_2-coated (c, d) $Y_2O_3:Tb^{3+}$ (2 at %).

Europe PMC Funders Author Manuscripts

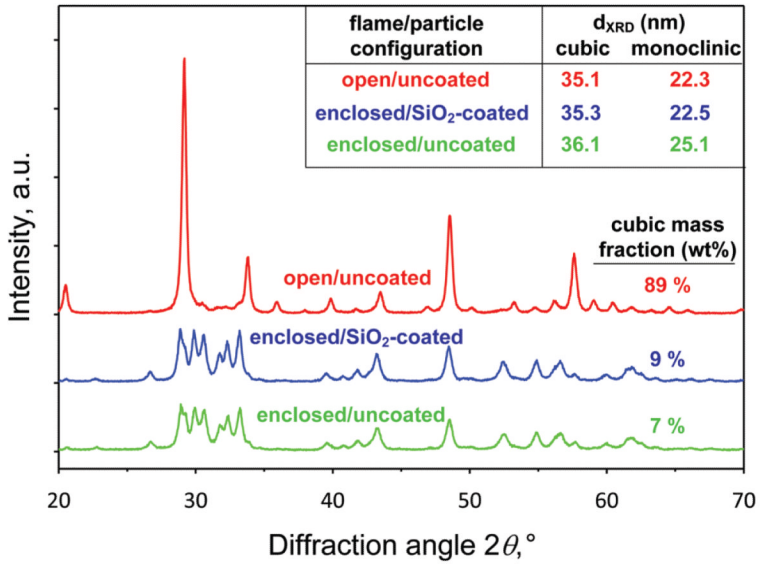

Figure 2.

X-ray diffraction patterns of open uncoated, enclosed uncoated, and enclosed SiO_2-coated Y_2O_3:Tb^{3+} (2 at %). The open FSP made Y_2O_3:Tb^{3+} nanoparticles exhibit the characteristic cubic crystal structure, while both enclosed FSP made nanoparticles exhibit the monoclinic Y_2O_3 crystal structure. The average crystal sizes of the cubic and monoclinic phases and the corresponding mass fraction of the cubic phase are also shown.

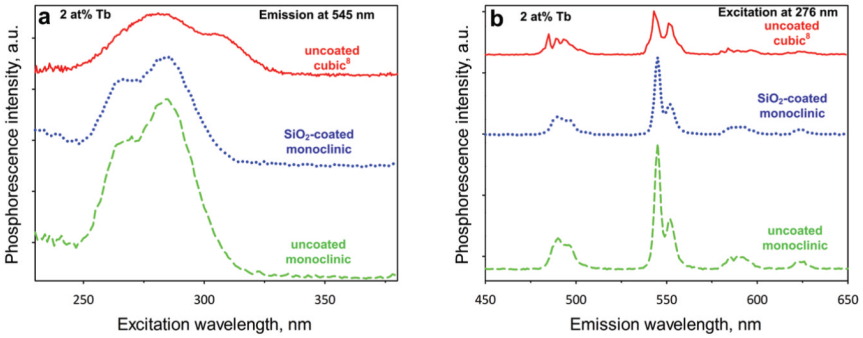

Figure 3.

(a) The excitation spectra of the 2 at % Tb-doped Y_2O_3 uncoated cubic (solid line), uncoated monoclinic (broken line), and SiO_2-coated monoclinic (blue line) nanoparticles monitored at 545 nm. The two bands around 280 and 310 nm are attributed to Tb^{3+} transitions. (b) Emission spectra of the same samples under 276 nm excitation. The appearing peaks correspond to Tb^{3+} ion transitions, with the most dominant being the one at 545 nm attributed to the $^5D_4 \rightarrow {}^7F_5$ transition.

Europe PMC Funders Author Manuscripts

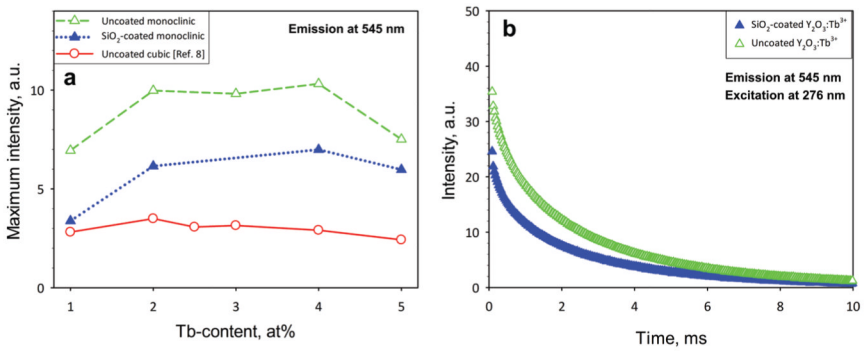

Figure 4.

(a) The maximum phosphorescence intensity monitored at 545 nm under excitation of 276 nm for the uncoated cubic (solid line, open circles) from ref 8, uncoated monoclinic (broken line, open triangles), and SiO_2-coated monoclinic (dotted line, filled triangles) nanoparticles as a function of Tb content. (b) Photoluminescence emission intensity decay curves of as-prepared, uncoated (open triangles), and SiO_2-coated (filled triangles) Y_2O_3:Tb^{3+} (2 at % Tb) nanophosphors.

Europe PMC Funders Author Manuscripts

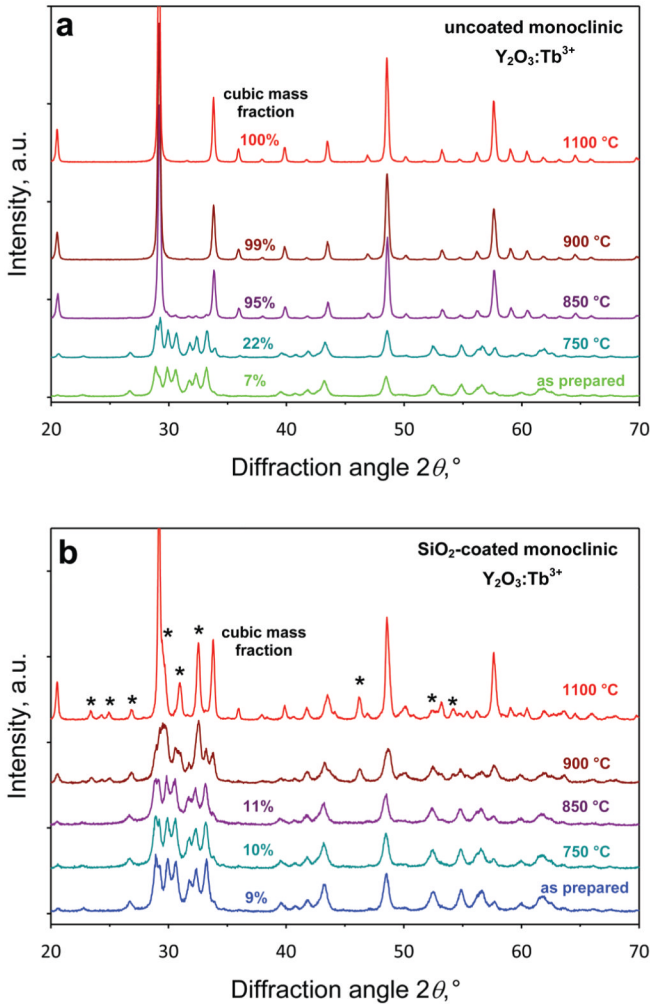

Figure 5.

XRD patterns of the uncoated monoclinic (a) and SiO_2-coated monoclinic (b) Y_2O_3:Tb^{3+} (2 at % Tb) for different annealing temperatures (750, 850, 900, and 1100 °C) for 10 h. For the uncoated nanoparticles, the transition from the monoclinic phase to cubic occurs for temperatures >850 °C, while the SiO_2 coating prevents this transition significantly until 900 °C. The stars indicate peaks that correspond to yttrium-silicates.

Europe PMC Funders Author Manuscripts

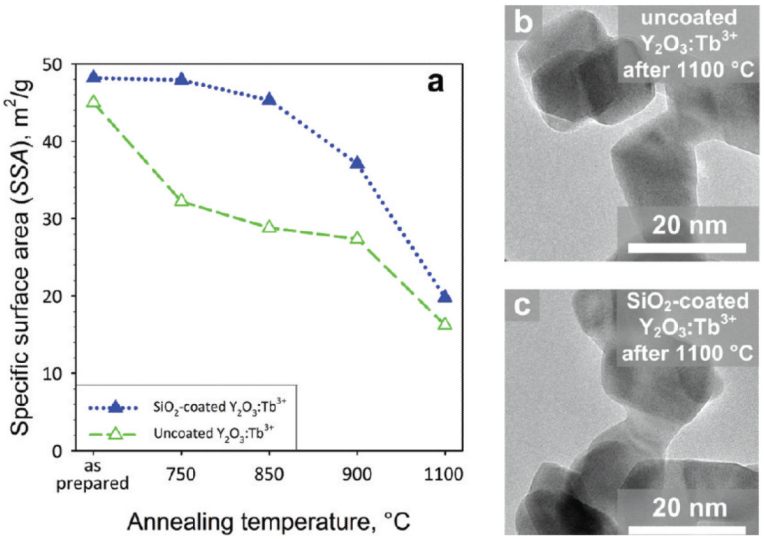

Figure 6.

(a) The specific surface area (SSA) as a function of the annealing temperature for the uncoated (open triangles) and SiO_2-coated monoclinic (filled triangles) Y_2O_3:Tb^{3+} nanophosphors. TEM images of the uncoated (b) and SiO_2-coated (c) Y_2O_3:Tb^{3+} after 1100 °C annealing.

Europe PMC Funders Author Manuscripts

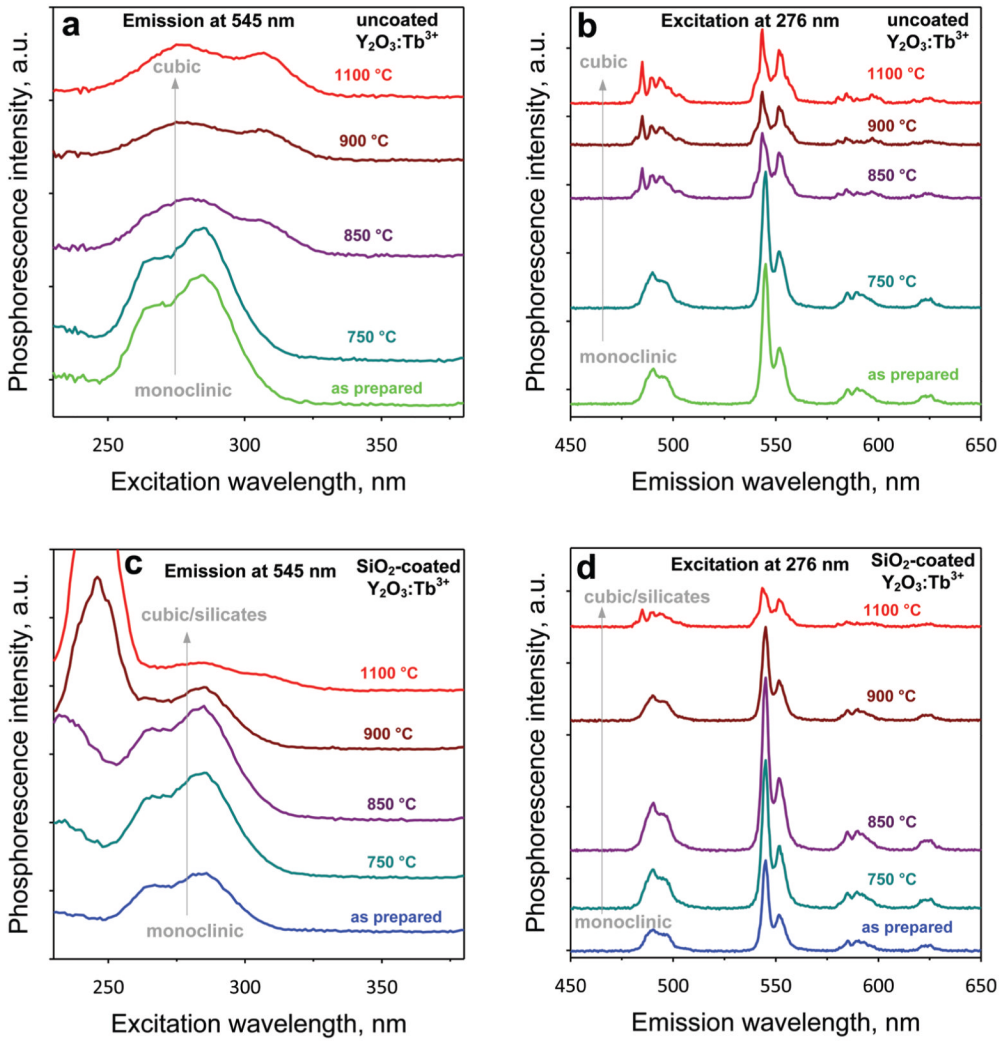

Figure 7.

The excitation monitored at 545 nm (a, c) and emission under 276 nm excitation (b, d) spectra of the 2 at % Tb-doped Y_2O_3 uncoated monoclinic (a, b) and SiO_2-coated monoclinic (c, d) nanoparticles for the different annealing temperatures (750, 850, 900, and 1100 °C). The phosphorescence intensity decreases for the transition from monoclinic to cubic crystal structure.

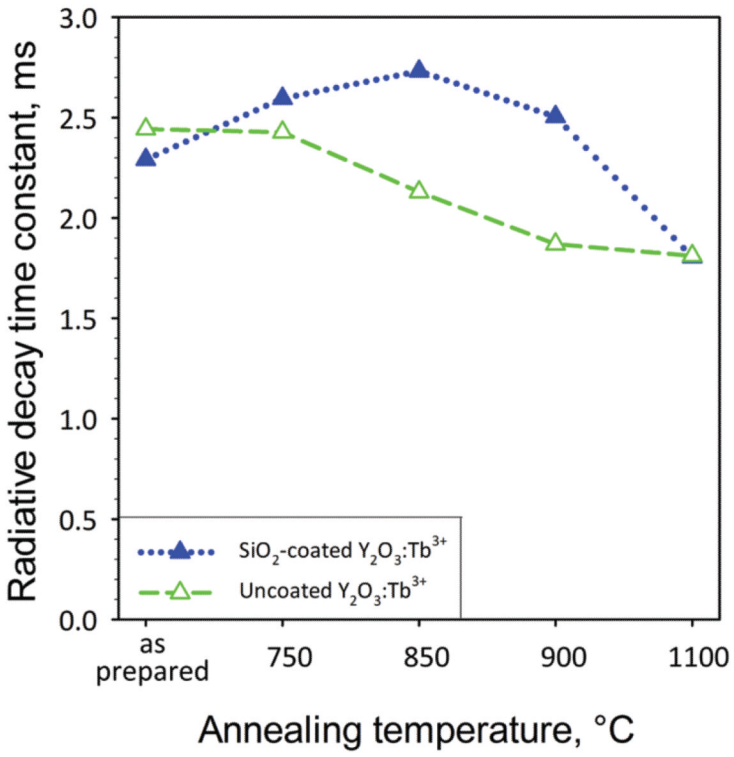

Figure 8.
The exponential decay time constants of luminescence for the uncoated (open triangles) and SiO_2-coated (filled triangles) Y_2O_3:Tb^{3+} (2 at % Tb) as a function of the annealing temperature.

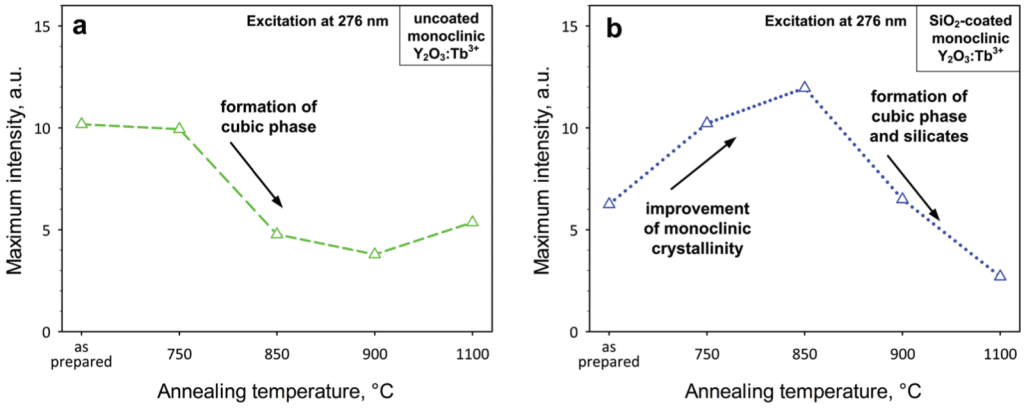

Figure 9.

The maximum phosphorescence intensity of the uncoated (a) and SiO_2-coated (b) monoclinic $Y_2O_3:Tb^{3+}$ (2 at % Tb) nanophosphors when excited at 276 nm for the different annealing temperatures.

Europe PMC Funders Author Manuscripts